The Fatigue of Aluminum Alloys Subjected to Random Loading

Experimental investigation is undertaken by the authors to determine the fatigue life of 2024-T3 and 6061-T6 aluminum alloys

G. W. Brown and R. Ikegami

ABSTRACT—This paper describes an experimental investigation which was carried out to determine the fatigue life of two aluminum alloys (2024-T3 and 6061-T6). They were subjected to both constant-strain-amplitude sinusoidal and narrow-band random-strain-amplitude fatigue loadings. The fatigue-life values obtained from the narrow-band random testing were compared with theoretical predictions based on Miner's linear accumulation of damage hypothesis.

Cantilever-beam-test specimens fabricated from the aluminum alloys were subjected to either a constant-strain-amplitude sinusoidal or a narrow-band random base excitation by means of an electromagnetic vibrations exciter. It was found that the ϵ-N curves for both alloys could be approximated by three straight-line segments in the low-, intermediate- and high-cycle fatigue-life ranges. Miner's hypothesis was used to predict the narrow-band random fatigue lives of materials with this type of ϵ-N behavior. These fatigue-life predictions were found to consistently overestimate the actual fatigue lives by a factor of 2 or 3. However, the shape of the predicted fatigue-life curves and the high-cycle fatigue behavior of both materials were found to be in good agreement with the experimental results.

Symbols

b_1, b_2 = constants
k_1, k_2 = constants
N = number of cycles to failure
S = stress
S_y = yield stress
(ϵ_1, N_1) = reference point on ϵ-N diagram
ϵ = strain
ϵ_y = yield strain
ϵ_p = peak strain
ϵ_e = endurance-limit strain
η = strain-hardening exponent
σ_ϵ^2 = strain variance

Symbols not shown here are defined in the text.

G. W. Brown is Professor of Mechanical Engineering, University of California, Berkeley, Calif. R. Ikegami is Research Engineer, Structural Dynamics Group, Boeing Aircraft, Seattle, Wash.

Paper was presented at 1970 SESA Spring Meeting held in Huntsville, Ala. on May 19–22.

Introduction

The problem of predicting the fatigue lives of metal structures which are subjected to random loadings is generally solved by first formulating an accumulation of damage criteria, then applying this criteria to the specified conditions of varying cyclic-load amplitude. The first and still the most commonly used criterion for predicting the accumulation of damage in fatigue was proposed by A. Palmgren and applied by M. A. Miner.[1] This criterion assumes that the problem of accumulation of damage may be treated as one in which the fractions of fatigue life used up at different load levels as determined from the constant amplitude ϵ-N curve may be simply added to give an index of the fatigue damage and is generally known as Miner's linear-accumulation-of-damage criteria.

This paper describes a portion of the results of a study[2] which was conducted to determine a method of predicting the fatigue lives of alumimum-alloy structures which were subjected to narrow-band random loadings. An experimental program was carried out to determine the lives of cantilever-beam test specimens which were subjected to either constant-strain-amplitude sinusoidal or narrow-band random strain-amplitude fatigue loadings. The fatigue lives of the test specimens subjected to the random loadings were then compared to predictions based on the application of Miner's criteria.

Experimental Program

The fatigue tests were performed on two commonly used aluminum alloys, 2024-T3 and 6061-T6. The mechanical properties of these two alloys are

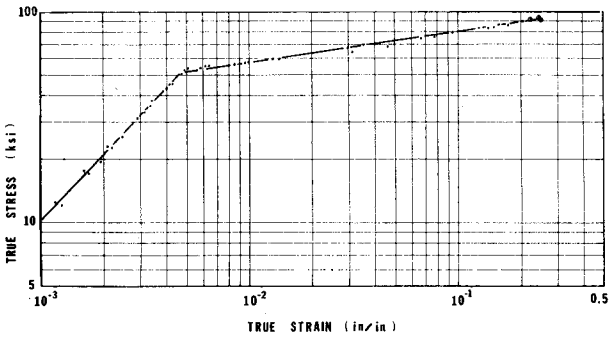

Fig. 1—True stress vs. true strain for 2024-T3 aluminum

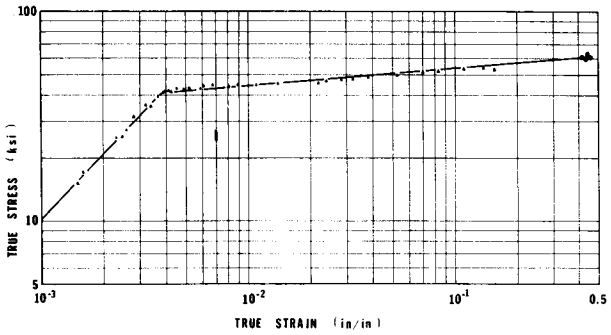

Fig. 2—True stress vs. true strain for 6061-T6 aluminum

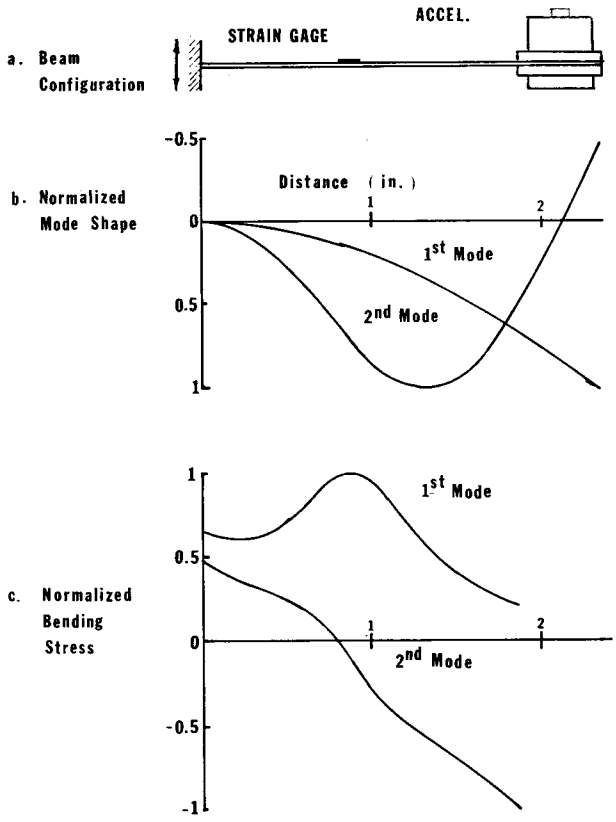

Fig. 3—Vibration characteristics of fatigue specimen

given in Table 1, and the true-stress vs. true-strain curves are shown in Figs. 1 and 2.

The strain-hardening exponent, η, characterizes the stress–strain relationship in the plastic range.

$$S = S_y \left(\frac{\epsilon}{\epsilon_y}\right)^{\eta}$$

These properties were determined from uniaxial tensile tests using tension specimens made from the two alloys. In both cases, the tension specimens and the fatigue specimens were machined from the same sheets of aluminum, with the longitudinal axes of the specimens parallel to the direction of rolling. This was done to insure uniformity between these two types of tests.

The majority of the fatigue tests was done on an electromagnetic vibrations exciter, with a small portion of the low-cycle constant-strain-amplitude tests being performed on an Instron tester.

For the testing which was performed on the vibrations exciter, the fatigue-test model was a cantilever beam subjected to a base excitation, as shown schematically in Fig. 3(a). For the narrow-band random fatigue tests, the excitation was a narrow-band signal with a Gaussian base-acceleration amplitude and uniform spectrum over a specified frequency bandwidth. The excitation band was centered at the fundamental beam resonance. The sinusoidal fatigue tests were performed with the excitation frequency slightly above the fundamental beam resonance. The type of cyclic loading was therefore completely reversed bending.

The cantilever specimens were profiled along the length of the beam to move the maximum bending stress in the first mode of vibration away from the fixed end. A sketch of the test-specimen configuration is shown in Fig. 4. The test specimens were clamped in the middle by a mounting fixture which was attached directly to the armature of the vibrations exciter. As can be seen from the figure, each fatigue-test specimen contained two cantilever-beam specimens which were excited simultaneously. An end mass, in the form of an Endevco Model 2216 crystal accelerometer, was attached at the free end of the cantilever-beam specimens. The mode shapes and corresponding bending-stress distributions for the first two modes of vibration are shown in Figs. 3(b) and 3(c). At the fundamental beam resonance, the maximum bending stress occurred at

TABLE 1—MATERIAL PROPERTIES

Material	Elastic modulus, psi	Yield stress, psi	True fracture stress, psi	True fracture strain, in./in.	Strain-hardening exponent
2024-T3	10.6×10^6	51,000	90,700	0.240	0.147
6061-T6	10.6×10^6	40,500	62,000	0.440	0.0875

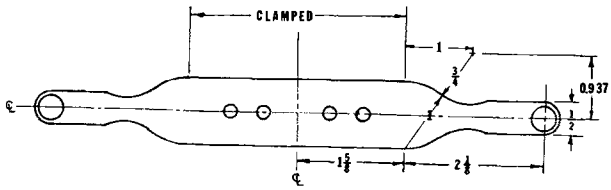

Fig. 4—Fatigue-test specimen

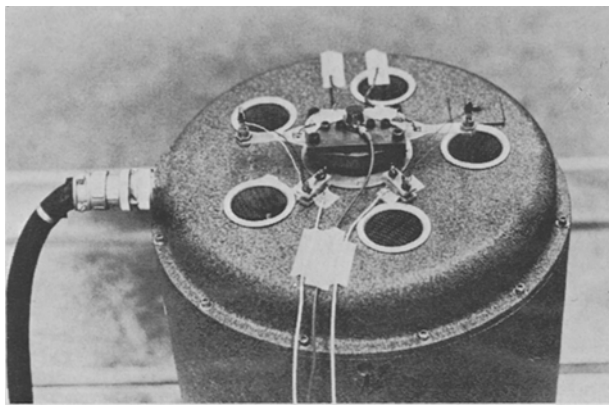

Fig. 5—Fatigue specimen on vibration exciter

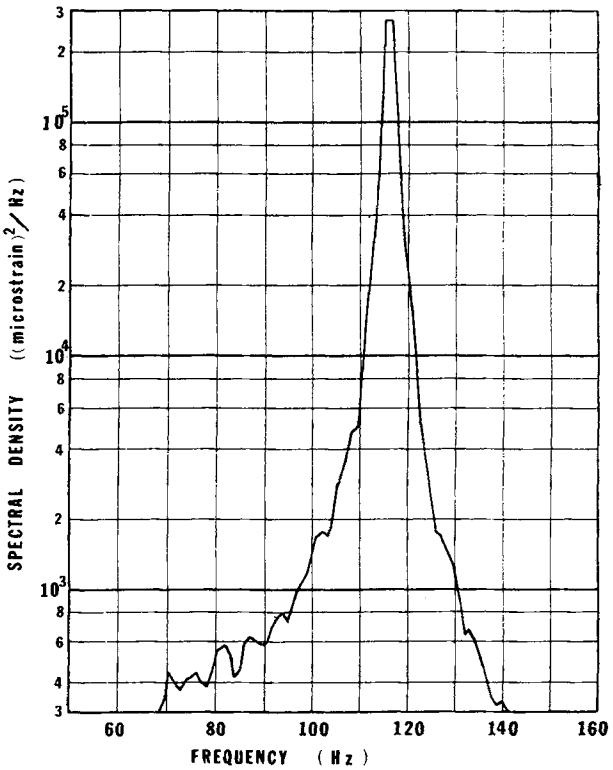

Fig. 6—Strain spectral density

a distance of $^{7}/_{8}$ in. from the fixed end of the beam. The frequency of the first beam resonance was approximately 115 cps. The specimens were carefully hand polished prior to testing to remove any sharp corners and to eliminate all visible surface scratches in the region in which the maximum stress occurred.

To measure the strain level during the fatigue tests, strain gages were mounted on every specimen at the point where the maximum bending stress occurred. It was found that the fatigue life of the strain-gage installation was generally much smaller than the fatigue life of the specimen. For this reason, the signal from the accelerometer mounted at the free end of the beam was used to determine the time to failure of the fatigue specimens. The signal from the accelerometer was used to trigger a relay which deactivated a timer when the acceleration level dropped to 50 percent of the nominal RMS acceleration level. It was observed that, at failure, the acceleration level dropped very rapidly so that the timers indicated very closely the total time to failure of the specimen.

The picture in Fig. 5 shows a fatigue-test specimen mounted on the vibrations exciter just prior to testing. As can be seen from this figure, special accelerometer cables were constructed by splicing standard Microdot accelerometer cables with two smaller, more flexible, lead wires. This was done to minimize the effect of the vibrations of the accelerometer cable on the specimen. Although the splice increased the noise pickup, the signal level was so large that this increase in noise was not noticeable.

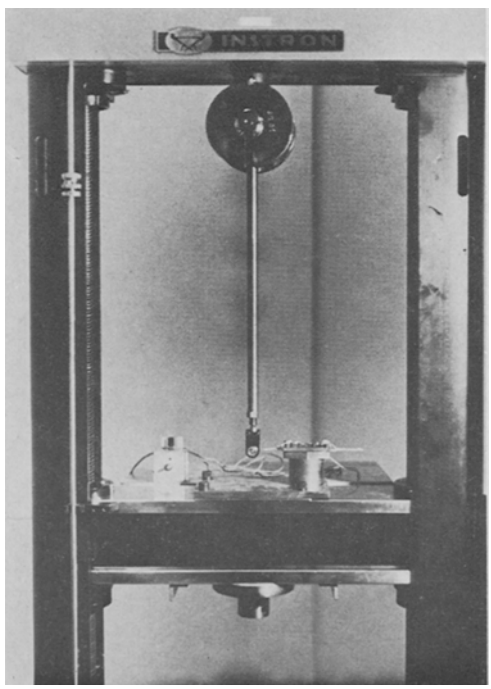

Fig. 7—Fatigue specimen in Instron tester

The signals from the strain gages and the accelerometers were monitored during the tests and recorded on magnetic tape. After each test, the recorded signals were played back into a wave-

analyzer system to determine the RMS levels. A digital computer was used to perform a time-series analysis of the random signals obtained from the narrow-band random fatigue tests. A strain spectral-density plot of the strain-gage response during a typical narrow-band random test is shown in Fig. 6. As expected, this plot indicates that the fatigue specimen can be considered to be a very lightly damped, single-degree-of-freedom system. The most probable frequency of vibration of this narrow-band response can be shown to be the resonance frequency of the system. Therefore, the total number of cycles to failure (i.e., the total number of zero crossings with positive slope) was assumed to be the total time to failure in seconds multiplied by the resonance frequency in cycles per second. In the constant-amplitude, sinusoidal tests the total number of cycles to failure was merely the total time to failure in seconds multiplied by the excitation frequency in cycles per second.

For the tests performed on the vibrations exciter, the range of the total cycles to failure was from 2×10^3 to 5×10^7 cycles. The corresponding strain levels ranged from 600 to 3500 microstrain RMS for the narrow-band random fatigue tests, and from 1700 to 7000 microstrain for the constant-amplitude testing.

Due to the fast rate of cycling on the vibrations exciter, it was not possible to obtain fatigue data for life values below approximately 2×10^3 cycles using the test setup described above. For this reason, some low-cycle, constant-strain-amplitude fatigue testing was performed on an Instron tester. A knowledge of the low-cycle, constant-amplitude

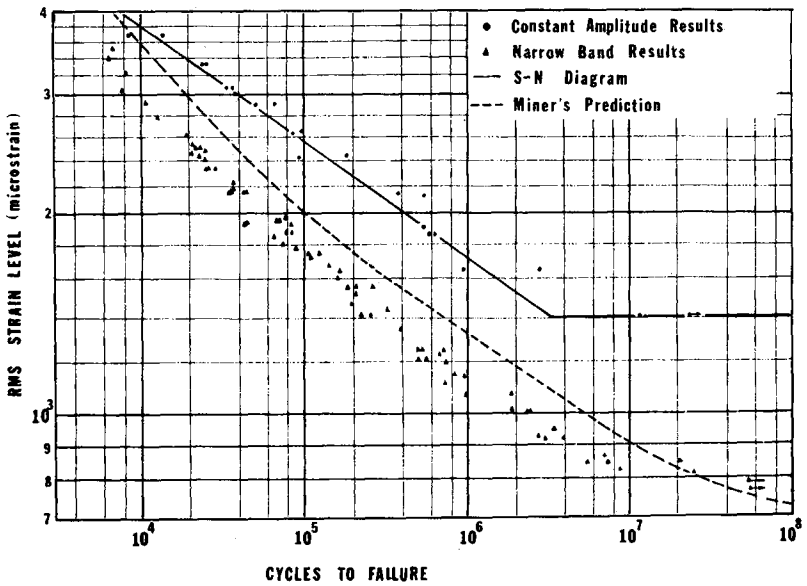

Fig. 8—Fatigue-test results for 2024-T3 aluminum

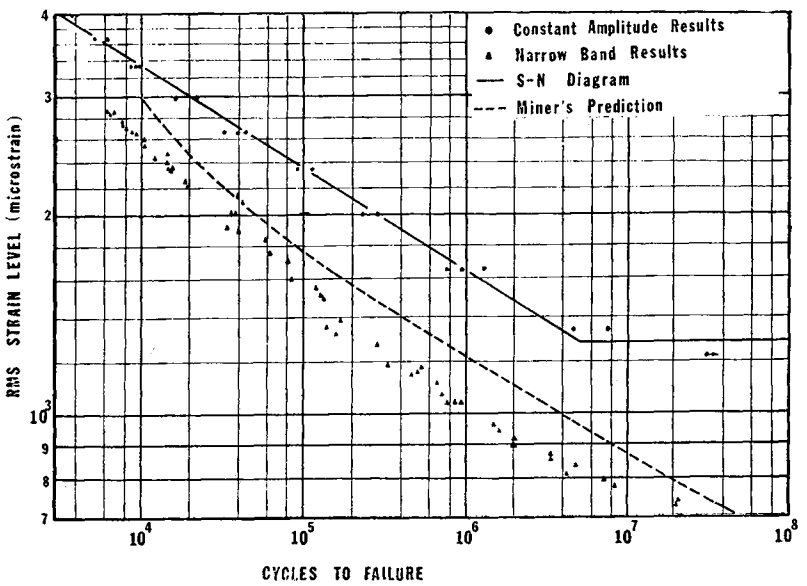

Fig. 9—Fatigue-test results for 6061-T6 aluminum

fatigue behavior of the two materials is necessary to correlate the constant-amplitude and narrow-band random fatigue results using Miner's criteria. For a Rayleigh distribution, the probability of the peaks exceeding 3.72 times the RMS value is 0.1 percent. Since the highest RMS-strain level for the narrow-band random tests was 3500 microstrain, peak strain levels of approximately 14,000 microstrain could be expected. The vibrations exciter was capable of producing constant-amplitude peak strains of only 7000 microstrain; consequently, other means had to be employed to produce an ϵ-N diagram up to the 14,000-microstrain level required for Miner's prediction of failure. The Instron tester programmed to cycle at a rate of approximately 5 cpm with strain amplitudes of up to 40,000 microstrain was used to obtain the low-cycle data. The specimens again were loaded in completely reversed bending and were essentially the same as those used in the vibrations-exciter tests.

A photograph of the test setup for the Instron fatigue testing is given in Fig. 7. The test specimen was mounted on the crosshead of the Instron tester by means of a mounting fixture which held the specimen in the same manner that the specimens were held when mounted on the vibrations exciter. The tip of the specimen was held stationary by means of the two-force member which connected the tip to the frame of the testing machine. The base or crosshead was then cycled through a constant deflection. The number of cycles to failure was determined from a counter on the Instron tester.

The results of the fatigue tests performed on the vibrations exciter are shown in Figs. 8 and 9, where the RMS strain level has been plotted vs. the total number of cycles to failure of the cantilever-beam specimens. Both the constant-amplitude and the

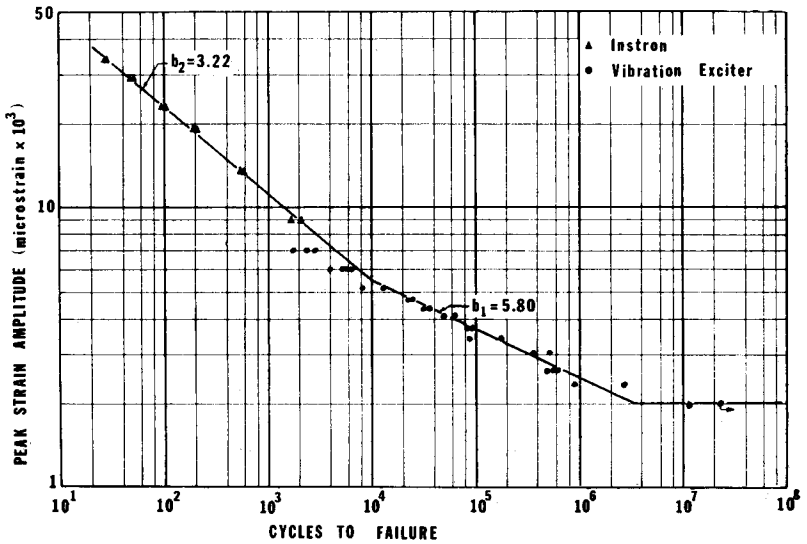

Fig. 10—Constant-amplitude fatigue-test results for 2024-T3 aluminum

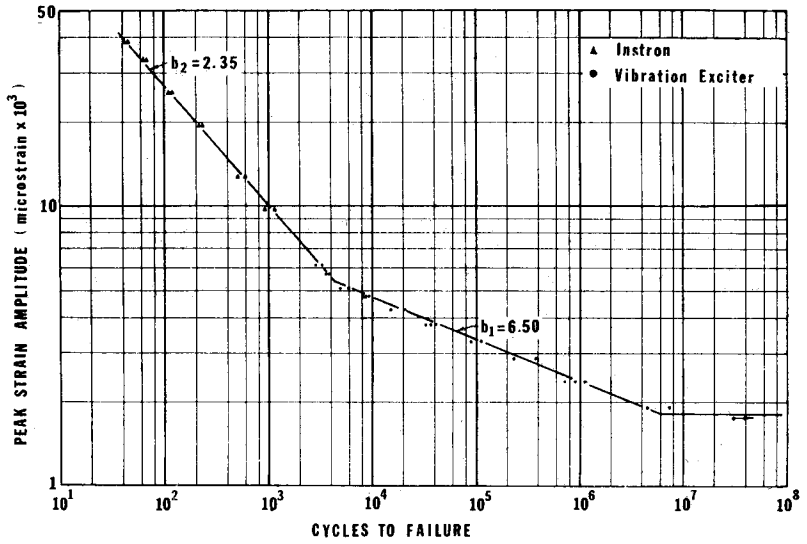

Fig. 11—Constant-amplitude fatigue-test results for 6061-T6 aluminum

narrow-band random results have been plotted on the same graph to emphasize the difference in fatigue life obtained with the two different types of loading at the same RMS strain level.

It can be noticed that both materials, when subjected to constant-strain-amplitude sinusoidal and narrow-band random strain-amplitude fatigue loads, exhibited an endurance-limit phenomenon at the very low strain levels. Most of the constant-amplitude data seems to fall on a straight line in the log-log plot of RMS strain amplitude vs. the total number of cycles to failure. Some deviation is indicated in the data for 6061-T6 at the high strain levels. This is to be expected since the strains corresponding to these points are well into the plastic region. It is believed that the 2024-T3 material would show the same type of deviation at higher strain levels than could be obtained with the existing vibrations-exciter test setup. The narrow-band random fatigue-test results show the same linear behavior on a log-log plot with a slope which is the same as the corresponding constant-amplitude data at the lower RMS strain levels. The data then begin to deviate at the higher strain levels where a greater number of strain peaks would be expected to exceed the yield strain.

The results of the constant-strain-amplitude fatigue tests performed on the Instron tester are shown in Figs. 10 and 11, where the amplitude of peak strain, ϵ_p, has been plotted vs. the total number of cycles to failure of the cantilever-beam specimens. The Instron test data are plotted with the constant-amplitude results from the vibrations-exciter tests. Since materials which exhibit a frequency effect generally show lower fatigue-life values as the cycling frequency is lowered,[3] it is believed that the difference in cycling frequency did not greatly affect the fatigue behavior of the two materials tested; consequently the two sets of data can be directly compared. It is generally believed that there is little significant effect when working with frequencies of up to about 1000 cps.[4]

From the results shown in Figs. 10 and 11 and the results of the tensile tests, it can be seen that a plot of stress amplitude vs. the number of cycles to failure would be of little use when large plastic strains are experienced. Due to the nature of the stress–strain relations in the plastic range, a large incremental increase in strain corresponds to a very small incremental increase in stress. Therefore, in this paper, either the RMS strain amplitude or else the amplitude of peak strain ϵ_p is plotted vs. number of cycles. The symbol ϵ_p is for peak strain, rather than for "plastic strain."

Figures 10 and 11 show that the low-cycle-fatigue data seem to fall on a straight line in a log-log plot of peak-strain amplitude vs. the number of cycles to failure. In both cases, the slope of this line is much greater than the slope of the line passing through the high-cycle data. These straight-line relationships on the log-log plots indicate that, for constant-strain-amplitude cycling, approximate relationships between the total number of cycles to failure and the peak-strain amplitude can be obtained in exponential form. In the high-cycle range, this relationship can be expressed as

$$N_f = k_1 \epsilon_p^{-b_1} \quad (1)$$

and in the low-cycle range as

$$N_f = k_2 \epsilon_p^{-b_2} \quad (2)$$

where k_1 and k_2 are constants. N_f is the number of cycles to failure at the peak strain amplitude ϵ_p. The values of b_1 and b_2 for both materials are given in Figs. 10 and 11 and in Table 2.

TABLE 2—PARAMETERS USED IN MINER'S CALCULATIONS

Material	b_1	b_2	N_1 cycles	ϵ_1 in./in.	ϵ_e in./in.
2024-T3	5.80	3.22	1.35×10^4	0.00510	0.00198
6061-T6	6.50	2.35	4.20×10^3	0.00545	0.00180

This change of slope in the low-cycle, high-strain-amplitude region is in agreement with the observations of numerous other experimenters. L. F. Coffin[5] has observed that for many materials, if the plastic-strain amplitude* is plotted vs. the number of cycles to failure, b_2 is approximately equal to 2.

Using the results of the constant-strain-amplitude fatigue tests, the results of the narrow-band random fatigue tests can be compared with a prediction based on Miner's linear-accumulation-of-damage hypothesis.

Miner's Linear-accumulation-of-damage Criteria

As was discussed previously, Miner's prediction of failure assumes that failure is due to a linear accumulation of damage which can be determined from the results of the constant-amplitude testing. The complete constant-amplitude results, including both

* *For this case, the plastic-strain amplitude would be the peak-strain amplitude minus the yield strain.*

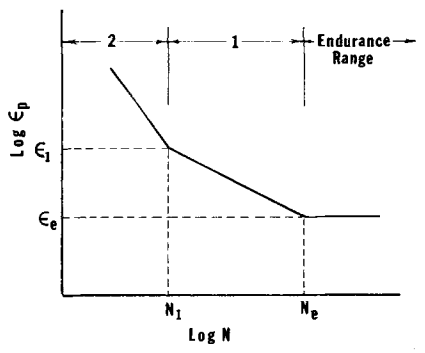

Fig. 12—Idealized ϵ-N diagram

the low- and high-cycle-fatigue life ranges, have been plotted in Figs. 10 and 11 for both of the materials tested. As can be seen from the figures, the ϵ-N curves for both materials can be approximated by three straight-line segments when plotted on a log-log scale. These three ranges can be indicated schematically as shown in Fig. 12.

In range 2, it will be assumed that the ϵ-N diagram is a straight line on a log-log plot from zero to N_1 cycles with a negative slope of $1/b_2$. In range 1, it will be assumed that the straight line extending from N_1 to N_e cycles has a negative slope of $1/b_1$. The horizontal line at ϵ_e corresponds to the endurance strain. It will be assumed that strains below this level have no influence on the final fatigue failure. Thus, the ϵ-N curve can be expressed as

$$[N(\epsilon_p)]_2 = N_1 \left(\frac{\epsilon_p}{\epsilon_1}\right)^{-b_2} \quad \text{for} \quad \epsilon_1 < \epsilon_p < \infty, \quad 0 \leq N \leq N_1 \tag{3}$$

and

$$[N(\epsilon_p)]_1 = N_1 \left(\frac{\epsilon_p}{\epsilon_1}\right)^{-b_1} \quad \text{for} \quad \epsilon_e \leq \epsilon_p \leq \epsilon_1, \quad N_1 \leq N \leq N^e$$

For this case, the linear-accumulation-of-damage equation can be written in terms of the peak-strain amplitude as

$$\text{Acc. Dam.} = M_o T \left[\int_{\epsilon_e}^{\epsilon_1} \frac{p_p(\epsilon_p) d\epsilon_p}{[N(\epsilon_p)]_1} + \int_{\epsilon_1}^{\infty} \frac{p_p(\epsilon_p) d\epsilon_p}{[N(\epsilon_p)]_2} \right] \tag{4}$$

where $p_p(\epsilon_p)$ is the probability density function of the peak-strain amplitude, T is total time to failure and M_o is the number of positive peaks per second. Thus $M_o T$ represents the total number of positive peaks to failure. Since the strain response is an extremely narrow-band process, the peak-strain probability density function resulting from the imposed Gaussian distribution in excitation is a Rayleigh distribution, and can be expressed as

$$p_p(\epsilon_p) = \frac{\epsilon_p}{\sigma_\epsilon^2} e^{-\epsilon_p^2/2\sigma\epsilon^2} \tag{5}$$

Using eqs (3), (4) and (5), the accumulation of damage is

$$\text{Acc. Dam.} = \frac{M_o T}{N_1 \sigma_\epsilon^2} \left[\frac{1}{\epsilon_1^{b_1}} \int_{\epsilon_e}^{\epsilon_1} \epsilon_p^{b_1+1} e^{-\epsilon_p^2/2\sigma\epsilon^2} d\epsilon_p + \frac{1}{\epsilon_1^{b_2}} \int_{\epsilon_1}^{\infty} \epsilon_p^{b_2+1} e^{-\epsilon_p^2/2\sigma\epsilon^2} d\epsilon_p \right] \tag{6}$$

Final failure is assumed to occur when the accumulation of damage is equal to unity so that the total number of positive peaks to failure is

$$M_o T = \frac{N_1 \sigma\epsilon^2}{\left[1/\epsilon_1^{b_1} \int_{\epsilon_e}^{\epsilon} \epsilon_p^{b_1+1} e^{-\epsilon_p^2/2\sigma\epsilon^2} d\epsilon_p + 1/\epsilon_1^{b_2} \int_{\epsilon_1}^{\infty} \epsilon_p^{b_2+1} e^{-\epsilon_p^2/2\sigma\epsilon^2} d\epsilon_p \right]} \tag{7}$$

The solution of this equation was programmed for a CDC 6400 digital computer. The parameters used in the calculations of Miner's prediction for the two materials which were tested are given in Table 2.

The predictions based on Miner's hypotheses are indicated by the dashed lines in Figs. 8 and 9. As can be seen from these figures, although the form appears to follow the trend of the data, Miner's prediction consistently overestimates the fatigue life by a factor of 2 or 3.

Conclusions

Resonance fatigue testing on an electromagnetic vibrations exciter seems to be a very fast, economical way of obtaining constant-strain-amplitude sinusoidal and random-strain-amplitude loading fatigue data. However, due to the high-cycling rates, low-cycle-fatigue data cannot be obtained in this manner.

For the aluminum alloys tested, there appear to be three distinct fatigue ranges corresponding to the three different line segments required to fit the ϵ-N data plotted on a log-log scale. To apply Miner's criteria to the prediction of fatigue lives under narrow-band random-loading conditions, the ϵ-N data must be complete to a strain level of at least four times the RMS strain level of the random loading.

Predictions based on Miner's criteria appear to consistently overestimate the actual fatigue lives; however, the form of the predicted curve appears to be correct and follow the trend in the data very closely.

Acknowledgment

This study was sponsored by Sandia Corporation of Livermore, Calif., under contract number 18-4278.

References

1. *Miner, M. A., "Cumulative Damage in Fatigue," Trans. of ASME Jnl. Appl. Mech., 87 (2), 159 (1945).*
2. *Brown, G. W. and Ikegami, R., "The Fatigue of Aluminum Alloys Subjected to Random Loadings," Rep. No. MD-69-1, Univ. of California, College of Engineering, Berkeley, Calif. (January 1969).*
3. *Harris, W. J., Jr., "Metallic Fatigue," Int. Series of Monographs in Aeronautics and Astronautics, Pergamon Press, New York (1961).*
4. *Kennedy, A. J., "Processes of Creep and Fatigue in Metals," Oliver and Boyd, Ltd., Edinburgh, Great Britain (1962).*
5. *Coffin, L. F., Jr., "Low-Cycle Fatigue: A Review," Appl. Mater. Res., 1 (3), 129 (October 1962).*
6. *Bendat, J. S., "Principles and Applications of Random Noise Theory," John Wiley & Sons, Inc., New York (1958).*
7. *Robson, J. D., "An Introduction to Random Vibrations," Edinburgh University Press, Edinburgh, Great Britain (1964).*